Optimizing HVAC Operations in Multi-unit Buildings for Grid Demand Response

Syed Ahsan Raza Naqvi*, Koushik Kar*, Saptarshi Bhattacharya† and Vikas Chandan†
*Rensselaer Polytechnic Institute, Troy, NY, USA, † Pacific Northwest National Laboratory, Richland, WA, USA.
Email: naqvis2@rpi.edu, koushik@ecse.rpi.edu, saptarshi.bhattacharya@pnnl.gov, vikas.chandan@pnnl.gov

Abstract—The thermal inertia of buildings, along with the flexibility associated with thermostatically controlled loads (TCL) allows heating, ventilation and cooling (HVAC) systems to be used for grid demand response (DR). In this work, we consider a hydronic HVAC system that serves multiple units in a residential building to meet their space heating requirements. We aim to determine the optimal power flow to each unit that minimizes the power costs incurred by the building's occupants while keeping in consideration their thermal comfort. The DR program is assumed to allow the building temperatures to deviate from the set-points up to a maximum limit. Despite the complex, non-linear structure of the problem, we show how the optimal solutions can be obtained efficiently using quadratic programming. Since HVAC systems can run on either electricity or natural gas, we study the efficacy of the DR regime for both hourly electricity prices and flat gas prices over the course of 24 hours. We also study the optimal thermal power and the evolution of unit temperatures for various energy pricing schemes.

I. INTRODUCTION

Heating, ventilation and cooling (HVAC) systems accounted for approximately 30% of the total energy consumed by the commercial building sector in the United States in 2017 [1]. According to another report [2], 56% of all energy consumed in homes in the state of New York in 2009 was used for space heating alone. Since a large part of the country consistently experiences winter temperatures close to freezing point, domestic heating requirements can rise substantially. This in turn leads to an increase in demand for electricity and gas. In response, system operators have to ramp up generation which is often achieved by turning on peaking power plants. These plants are not only expensive to operate but are also environmentally polluting. The higher running costs for such plants result in higher hourly prices paid by the consumers. Demand response (DR) in buildings is one possible way among many others to prevent elevated energy costs. In this paper, we focus on DR-compliance for the HVAC systems in residential complexes. The slow thermal dynamics and hence the thermal storage capabilities of buildings mean that in the presence of an adequate control scheme, heating loads can be shifted or curtailed, although at the cost of some thermal discomfort to the occupants [3].

Recently, the use of DR for load shifting and load curtailment in HVAC systems has received increased attention among researchers. The prospects of employing DR in both commercial and residential HVAC systems have been studied. The authors in [3] aimed to ascertain the potential of introducing DR programs to HVAC systems in residential areas. The DR was implemented using a deadband which represented the occupants' tolerance to variation in the indoor temperature. Unlike our work, the authors in [3] did not consider the role of energy prices in the effectiveness of DR in their study.

Some DR programs may use real-time pricing (RTP) as a means to shift the demand to low load, low price periods. The authors in [4] studied price-based DR strategies for controlling electric space heating loads using a hardware-in-the-loop framework. In [5], the authors proposed a load management strategy for HVAC systems which was based on model predictive control (MPC) using a data-driven approach to model the thermal dynamics of the building. Unlike [5], we consider a multi-unit residential building, and a physical model for a hydronic (water-based) HVAC system. One benefit of using a physics-based model is that with some modification, this model can potentially be applied to other HVAC systems as well.

In this work, we consider a hydronic HVAC system that serves multiple units in a residential building to meet their space heating requirements, as shown in Fig. 1. With each unit having a temperature set-point, we aim to determine the optimal mass flow of the heated water to each unit that minimizes the weighted sum of the thermal discomfort and the energy costs incurred over a time horizon. This paper considers three power pricing schemes: flat, time-of-use (ToU), and hourly. The flat pricing scheme represents the situation where the boiler is heated by natural gas. On the other hand, the ToU and the hourly pricing schemes are applicable to electricity-powered HVAC systems. We assume that the DR program allows the building temperatures to deviate from the set-points to within a certain range, as agreed upon by the building operator and the power utility. We develop mathematical expressions for modeling the temperature evolution in residential units over time. Despite the complex, apparent non-convex structure of the problem, we show how the optimal solutions can be obtained using quadratic programming. Finally, we use our model to run simulations to determine the optimal thermal power and the evolution of unit temperatures for the three energy pricing schemes. Our initial results show that our solution may have a strong potential for saving significant electricity cost by using buildings for grid DR.

The rest of this paper is organized as follows: Section II provides details of the system model and poses our proposed control strategy as an optimization problem; Section III reformulates the problem by expressing the variables in terms of known constants and the supplied power; Section

Notation	Description
$\mathcal{J}$	set of all units in a building
Δ_j	temperature set-point for unit j
τ	the length of the entire time horizon
μ	duration of each time slot
K	total number of time slots $(= \frac{\tau}{\mu})$
$P_j(t)$	power consumed by unit j at time t
$T_j(t)$	zone temperature of unit j at time t
$P^{\text{total}}(t)$	total power consumed by all units at time t
w	weighting parameter
$\pi(t)$	energy price at time t
C_j	thermal capacitance of unit j
R_j	thermal resistance of unit j
$T_\infty(t)$	ambient temperature at time t
$\dot{m}_j(t)$	mass flow rate of the heated water towards unit j at time t
ρ	maximum permitted deviation from the temperature set-point
S_p	specific heat capacity of water
h_R	heat exchange coefficient
T_S	temperature of the supplied water
$T_{R,j}(t)$	temperature of the water returning from unit j at time t
$T_R(t)$	temperature of the water returning to the boiler at time t

TABLE I: Table of notations.

IV provides a discussion on the simulation results. Finally, Section V summarizes the findings of this paper.

II. PROBLEM FORMULATION

In this work we consider a set of units $\mathcal{J}$ located in a residential building. Each unit j has a pre-determined temperature set-point, Δ_j. Furthermore, ρ represents the maximum permitted temperature swing about Δ_j. This 'deadband' represents the flexibility in the HVAC load that is needed for implementing a DR program. The building is taken to be equipped with valves that can control the mass flow rate of the water depending on the heating requirements of each individual unit. We assume that the temperature of each unit is uniform. We use a typical R-C model to represent the thermal properties of the indoor units. It is further assumed that the these thermal parameters are known to (or well-estimated by) the utility. The HVAC system is assumed to operate at 100% efficiency, i.e., all the power used to heat up the water is converted to thermal power for heating the units[1]. The power consumed to heat up unit j at time t is given by $P_j(t)$. The space temperature of each unit is denoted by $T_j(t)$. Furthermore, $P^{\text{total}}(t)$ is the total thermal power required to heat up all the units at time t.

We consider a hydronic HVAC system in which heated water is distributed from a central source to spaces within

[1]Without loss of generality, we consider a heating scenario although our model and analysis extend to cooling as well.

a building (or part of a building). We take the central source to be a boiler which may be heated by either natural gas or electricity. The temperature of the water leaving the boiler is denoted by T_S and is assumed to be constant for the entire time horizon. The living spaces are heated using fan coil units. The HVAC system is equipped with valves to control the mass flow rate of water at time t, $\dot{m}_j(t)$, to the fan coil unit in space j. The temperature of the water returning to the boiler at time t is denoted by $T_{R,j}(t)$. Fig. 1 shows a simplified schematic of the HVAC system being studied here.

We pose our objective as an optimization problem that aims to minimize the weighted sum of (i) total energy costs for the consumers and (ii) the thermal discomfort experienced in all units over the entire time horizon. Mathematically, the objective is to minimize,

$$\int_0^\tau \{w\pi(t)P^{\text{total}}(t) + (1-w)\sum_{j\in\mathcal{J}}[T_j(t)-\Delta_j]^2\}dt, \quad (1)$$

subject to,

$(\text{C}'_1) \quad \dot{T}_j(t) = \frac{1}{C_j R_j}[T_\infty(t) - T_j(t)] + \frac{1}{C_j}P_j(t),$

$(\text{C}'_2) \quad P_j(t) = \dot{m}_j(t)S_p(T_S - T_{R,j}(t)),$

$(\text{C}'_3) \quad P_j(t) = h_R\Big(\frac{T_S + T_{R,j}(t)}{2} - T_j(t)\Big),$

$(\text{C}'_4) \quad 0 \le \dot{m}_j(t) \le \frac{1}{\phi_j},$

$(\text{C}'_5) \quad -\rho \le T_j(t) - \Delta_j \le \rho,$

where w and $\phi_{S,j}$ are constants and τ is the duration of the time horizon. The initial temperature of unit j is $T_j(0) = T_j^0$. Additionally, $\pi(t)$ denotes the energy price at time t. Let C_j and R_j represent the thermal capacitance and resistance, respectively, of unit j. Moreover, $T_\infty(t)$ is the ambient temperature at time k and is assumed to be known *a priori*. Let S_p be the specific heat capacity of water. Furthermore, T_S is the constant temperature of the water at the energy source, whereas $T_{R,j}(t)$ is the temperature of the water returning from the building at time t. Finally, h_R is a constant representing the heat exchange coefficient between water and air.

For the objective function in (1), (C'_1) models the evolution of unit j's temperature over time. Constraint (C'_2) links the power consumed with the mass flow rate and the change in temperature of the heating water. Constraint (C'_3) expresses the power consumed in terms of the heat exchanging coefficient and the temperature difference between the heating water and the surrounding air in the unit. The temperature of the water is approximated to be the average of the temperature of the supplied and returning water. Constraint (C'_4) enforces upper and lower bounds on $\dot{m}_j(t)$. Finally, constraint (C'_5) constrains the temperature swing about the set-point to be at most ρ.

The temperature of the water returning from the units to the boiler at time t is given by $T_R(t)$. This overall return temperature of the water can be obtained by the following equation:

$$T_R(t) = \frac{\sum_{j\in\mathcal{J}}\dot{m}_j(t)T_{R,j}(t)}{\sum_{j\in\mathcal{J}}\dot{m}_j(t)} \quad (2)$$
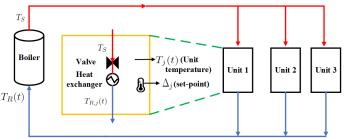
Fig. 1: Schematic of the hydronic HVAC system.

III. ANALYSIS

Inspecting the constraints for the objective in (1), we notice that (C'_2) makes the problem non-convex. Additionally, the problem contains several variables (like $\dot{m}_j(t)$, $P_j(t)$, $T_j(t)$ and $T_{R,j}(t)$) that must be determined optimally . Since we wish to study the efficacy of using residential TCLs for DR, we attempt here to reformulate our problem and express it in terms of a single control knob, $P_j(t)$. We also express $T_j(t)$ in terms of known constants and the supplied power. In the process, we express our problem as a convex (quadratic) problem with linear constraints. Towards that end, we first manipulate the constraint (C'_2) to give,

$$\frac{P_j(t)}{\dot{m}_j(t)S_p} = T_S - T_{R,j}(t). \tag{3}$$

Also, constraint (C'_3) can be manipulated to give,

$$2\left(\frac{P_j(t)}{h_R} + T_j(t)\right) = T_S + T_{R,j}(t). \tag{4}$$

Adding (3) and (4), we get,

$$\frac{1}{\dot{m}_j(t)} = \frac{2T_S S_p}{P_j(t)} - \frac{2S_p}{h_R} - \frac{2T_j(t)S_p}{P_j(t)}. \tag{5}$$

Using (C'_4) and setting $X_j(t) = \frac{1}{\dot{m}_j(t)}$, we get $\phi_j \leq X_j(t) < \infty$. We can then simplify (5) to be,

$$P_j(t) \leq G[T_S - T_j(t)], \tag{6}$$

where $G = \frac{2S_p}{\phi_j + \frac{2S_p}{h_R}}$ is a constant.

Following the manipulations above, our problem is simplified to minimizing (1) subject to constraints (C'_1), (C'_5) and (6). This results in two continuous variables, $T_j(t)$ (the state variable) and $P_j(t)$ (the control variable). However, in practice $\dot{m}_j(t)$, and hence $P_j(t)$, typically change only at discrete time intervals. Therefore, we can discretize the time scale for the valve operation into time slots. Each time slot is denoted by k and its duration is given by μ. We consider a total of K time slots where $K = \frac{\tau}{\mu}$. Thus, we express our control variable at time slot k as $P_j(k)$. Since the ambient temperature, T_∞, varies slowly, the variation within a time slot is expected to be small; so we represent it as a discrete variable $T_\infty(k)$.

It is noteworthy that using time-sampled versions of $T_j(t)$ can introduce significant errors in our computations. Therefore, we proceed to express the continuous-time state variable in terms of the discrete-time control variable. By modifying our existing notation and taking $k = \lfloor \frac{t}{\mu} \rfloor$, unit j's temperature

at time t is given by,

$$T_j(t) = H_{k,j}e^{-\frac{(t-k\mu)}{C_j R_j}} + T_\infty(k) + R_j P_j(k),$$
$$\text{for } t \in [k\mu, (k+1)\mu], \tag{7}$$

where

$$H_{k,j} = H_{0,j}e^{-\frac{k\mu}{C_j R_j}} + T_\infty(0)e^{-\frac{(k-1)\mu}{C_j R_j}}$$
$$+ \sum_{l=1}^{k-1} T_\infty(l)\left(e^{-\frac{(k-l-1)\mu}{C_j R_j}} - e^{\frac{-(k-l)\mu}{C_j R_j}}\right) - T_\infty(k) +$$
$$P_j(0)R_j e^{-\frac{(k-1)\mu}{C_j R_j}} + \sum_{l=1}^{k-1} P_j(l)\left(R_j e^{-\frac{(k-l-1)\mu}{C_j R_j}} - \right.$$
$$\left. R_j e^{-\frac{(k-l)\mu}{C_j R_j}}\right) - P_j(k)R_j. \tag{8}$$

The reader is directed to the detailed technical report of this paper [10] for further details of the derivation of (8).

In this work, we assume $P_j(0) = 0$. Moreover, as T_∞ and P_j only change at the slot boundaries, temperature $T_j(t)$ varies smoothly within the time slot. Therefore, it suffices to impose constraints (C'_5) and (6) only at the slot boundaries.

$$\sum_{k=1}^{K}\left\{w\pi(k)P^{\text{total}}(k) + (1-w)\sum_{j\in\mathcal{J}}\Upsilon_j(k)\right\}, \tag{9}$$

subject to,

(C_1) $\quad -\rho \leq T_j(k\mu) - \Delta_j \leq \rho, \quad\quad k \in [0,K],$

(C_2) $\quad P_j(k) \leq G[T_S - T_j(k\mu)], \quad\quad k \in [0,K],$

(C_3) $\quad T_j(k\mu) = H_{k,j} + T_\infty(k) + R_j P_j(k), \quad k \in [0,K],$

where

$$\Upsilon_j(k) = -\frac{C_j R_j H_{k,j}^2}{2}\left(e^{-\frac{2\mu}{C_j R_j}} - 1\right) +$$
$$\mu[T_\infty^2(k) + R_j^2 P_j^2(k) + 2T_\infty(k)R_j P_j(k)] -$$
$$2C_j R_j^2 H_{k,j}P_j(k)\left(e^{-\frac{\mu}{C_j R_j}} - 1\right) + \mu\Delta_j^2 -$$
$$2\mu\Delta_j[T_\infty(k) + R_j P_j(k)] - 2\Delta_j C_j R_j H_{k,j}\left(e^{-\frac{\mu}{C_j R_j}} - 1\right). \tag{10}$$

Further details on the derivation of (10) may be found in [10]. Note that the above formulation has been expressed in terms of only the discrete variable $P_j(k)$; all other time-dependent variables have been eliminated. It may be seen that the cost function for the optimization problem in (9) is quadratic and the constraints linear in $P_j(k)$. Once the optimal values for $P_j(k)$ have been determined for all $k \in [1,K]$, (7), (4) and
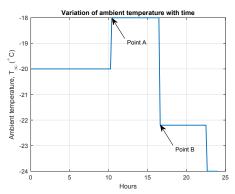
Fig. 2: Ambient temperature over a 24-hour period.

(3) may be used to obtain the unit temperatures, the return temperature of the water and the mass flow rate, respectively.

IV. NUMERICAL STUDY

Parameter	Value
C_j	4000 kJ $°C^{-1}$
R_j	5°C kW^{-1}
T_S	70° C
μ	10 min.
ϕ_j	1 kg s^{-1}
w	0.5
C_p	4200 J kg^{-1}
h_R	5 kW $°C^{-1}$

TABLE II: Simulation parameters and their values.

In this section, we use our model to run simulations to determine the optimal power and the evolution of unit temperatures for various energy pricing schemes. We consider a hydronic HVAC system that serves four units in a residential building. Let these units be given by j_1, j_2, j_3 and j_4. We assume that $\Delta_{j_1} = 21°C$, $\Delta_{j_2} = 23°C$, $\Delta_{j_3} = 25°C$, and $\Delta_{j_4} = 27°C$. It is further assumed that the building operator follows a DR program whereby the units' temperatures are allowed to vary within 2°C of their temperature set-points. The baseline case for our simulations is when $\rho = 0°C$, i.e., the scenario where the building operator does not participate in any DR program. The values for other simulation parameters may be found in Table II.

In January 2014, northeastern USA was affected by the 'Nor′easter' winter storm [6], resulting in ambient temperatures as low as -24°C. In the simulation results that follow, we use ambient temperatures observed on January 3, 2014 (see Fig. 2). This assumption enables us to observe the effectiveness of our control strategy under extreme weather conditions, which in turn result in high energy demand. We consider three energy pricing schemes for our HVAC system; flat, ToU and hourly (see Figs. 3a–3c). The flat energy prices refer to the scenario where the building's HVAC system uses natural gas, whereas the ToU and hourly prices are applicable to an electrical HVAC system (depending on which pricing scheme the power utility employs). The flat pricing scheme

used here reflects the average natural gas prices in the US in 2013 [7], whereas the hourly prices are based on New York independent system operator's (NYISO) day-ahead market prices for January 3, 2014 [8]. The ToU pricing scheme consists of two periods: the 'peak period' between 3 PM and 9 PM, and the 'off-peak period' for the rest of the day. As can be seen in Fig. 3b, the peak period has significantly higher energy prices than the off-peak period. While computing the optimal controls for our system, we assume that the prices are known (or are well-estimated) in advance.

Fig. 3 shows the effect of different pricing schemes on the total power consumed by the HVAC system and the average temperature deviation from the units' set-points, over a 24-hour period. Figs. 3d–3f present a comparison of the demand experienced by the grid when $\rho = 0°C$ and $\rho = 2°C$ for the three pricing schemes. Finally, Figs. 3g–3i depict the thermal discomfort experienced by the building's occupants when each of the three pricing schemes is employed.

We begin our analysis by studying the effects of the flat pricing scheme on the total power consumption of the building, as seen in Fig. 3d. The figure shows that the curves for both $\rho = 0°C$ and $\rho = 2°C$ exhibit largely identical trends over the 24-hour period. The constant energy prices mean that the power consumption in both cases is only responsive to the changing values of $T_\infty(k)$. For instance, the change in power consumption levels immediately before Points A′ and B′ in Fig. 3d are in response to the changing ambient temperatures at Points A and B in Fig. 2.

Fig. 3g shows the thermal discomfort (averaged over all units) experienced by the occupants of a DR-compliant residential building under the flat pricing. The figure shows that apart from the first hour, the average thermal discomfort remains constant at approximately 0.0045°C below the temperature set-point. The steady thermal discomfort levels can be attributed to the power consumption trend which is only affected by the ambient temperature when flat pricing is used.

Next, we study the effects of using ToU prices on the total power consumption of the building, as seen in Fig. 3e. Points C and D in Fig. 3b represents the beginning and end of the peak period, respectively. As is evident from Fig. 3e, for $\rho = 0°C$, the HVAC system is unaffected by the onset of the peak period as it has to strictly maintain the units' temperature at their set-points. The curve for $\rho = 0°C$ is only affected by the changes in $T_\infty(k)$. In contrast, the curve for $\rho = 2°C$ exhibits two regions of sharp increase in power consumption. One of these occurs just before the onset of the peak period, while the other occurs immediately after end of this peak period. The preheating phenomenon observed up to Point C′ in Fig. 3e exploits the slow thermal dynamic properties of the building to maintain the units' temperature within acceptable limits. Prior to the onset of the peak period, the HVAC system rapidly increases the supplied heat, while keeping in consideration the maximum allowable thermal discomfort. This operation results in no thermal power being supplied to the units between the time instances Point C′ and Point D′. Following the end of the peak period, the system once again ramps up the total power to approximately 580 kW. This allows the building to regain the thermal discomfort levels that were seen prior to the peak
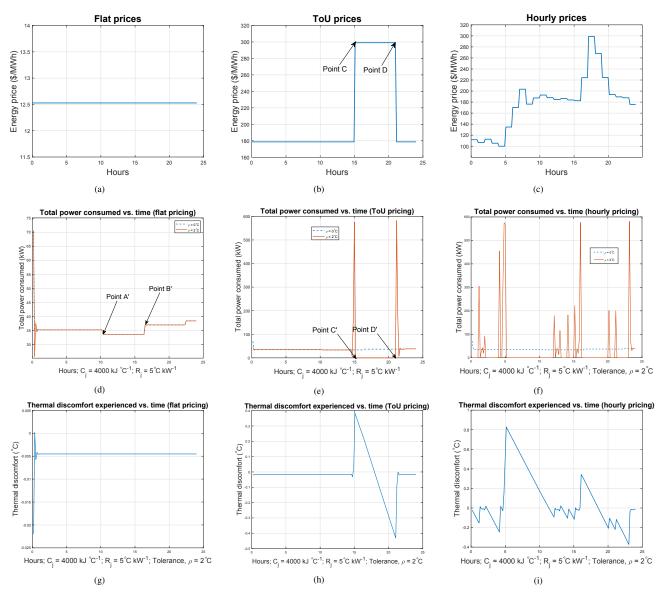
Fig. 3: (a)-(c): The three pricing schemes being studied. (d)-(f): The total power consumed by the units when a DR program is being implemented ($\rho = 2°C$) compared to the baseline scenario over a 24-hour period. (g)-(i): The thermal discomfort averaged over all units observed over a 24-hour period

| | % Financial Savings | Maximum temperature deviation (°C) | Peak-to-average power consumption | |
			$\rho = 0°C$	$\rho = 2°C$
Flat Pricing	0.15	0.02	1.97	1.98
ToU pricing	15.10	0.43	1.97	16.41
Hourly pricing	19.73	0.83	1.97	16.35

TABLE III: Effect of pricing schemes on various performance metrics.

period. Following this action, the curve for $\rho = 2°C$ follows a trend similar to that seen for $\rho = 0°C$.

Fig. 3h shows the change in average thermal discomfort over time for ToU pricing. The plot shows a steep rise in average thermal discomfort around hour 15. This is due to the preheating operation of the HVAC system that has previously been discussed. Since the HVAC system does not provide any heat between hours 15 and 21, hence the thermal discomfort increases in the opposite direction during this interval. Following a subsequent rise in power consumption, the thermal

discomfort is restored to the level seen in the off-peak period earlier.

Figs. 3f and 3i show the variation in the total power consumed and the average thermal discomfort for hourly prices. As before, the curve for $\rho = 0°C$ in Fig. 3f remains unaffected by the changes in energy price levels. The power consumption plot for $\rho = 2°C$, on the other hand, is characterized by (i) a series of 'spikes' of varying magnitudes and (ii) periods when no thermal power is supplied to the units. A steep rise in power consumption precedes any increase in the hourly prices. For

instance, the consumed power rises to approximately 570 kW prior to the rise in the energy prices after hour 5. This mode of operation reduces the supplied thermal power to 0 for periods of (relatively) high energy prices, as is the case for the interval between hours 5 and 12 and hours 16 to 20. Therefore, the HVAC system responds to the fluctuations in energy prices by consuming large amounts of power for short periods of time and relying on the building's ability to act as a storage buffer for heat to keep the thermal discomfort within permitted limits.

The plot for thermal discomfort versus time in Fig. 3i shows how thermal discomfort increases in the event of power spikes. The largest deviation from the temperature set-point was seen to be approximately $+0.81°C$. This value is due to the consistently high energy prices between hours 5 and 12, which causes the HVAC system to preheat the building. The intervals when the HVAC system shuts down witness an increase in the thermal discomfort in the negative direction.

Table III presents the expected % financial savings, maximum thermal discomfort and the peak-to-average ratios for the power consumed in the DR-compliant case for each of the three pricing schemes. The % financial savings have been determined with respect to the case when $\rho = 0°C$. The table shows that for flat pricing, DR-compliance results in negligible savings, compared to the case where no DR is used. This result was expected owing to the largely similar power consumption trends seen in Fig. 3d. The significantly higher % financial savings seen for the ToU and the hourly pricing schemes can be attributed to the preheating operation of the HVAC system. This mode of action helps restrict power consumption during intervals when the energy prices are relatively high. Therefore, our optimization strategy results in significant financial savings for DR-compliant electrical HVAC systems.

Table III also shows the maximum temperature deviation from the set-point for all three pricing schemes. It can be seen that for the energy price values used in this paper, the maximum temperature deviation for the hourly pricing is nearly twice that recorded for ToU pricing. This is due to the fact that the period of relatively high energy prices lasts longer for the hourly pricing scheme (hours 5 to 12) than for ToU pricing (hours 15 to 21). Therefore, hourly pricing causes the system to preheat the units to a greater extent. The table also records the peak-to-average ratio of the total power consumption for all pricing schemes when $\rho = 0°C$ and $\rho = 2°C$. It may be seen that this ratio is almost unaffected by the DR program when flat pricing is implemented. However, the preheating operation for both ToU and hourly pricing results in a much higher peak-to-average ratio in both cases. Although this paper's primary focus is to devise a control strategy for HVAC systems in DR-compliant residential buildings, the results for the peak-to-average ratio can offer interesting insights for larger users of electricity.

Commercial and industrial power consumers pay two types of tariffs in their electricity bill: one for the total energy used and another for the maximum demand in a particular window of time during the billing period [9]. The latter is called demand charge which is levied on a per-kW basis. The utility first determines the consumer's peak demand in a predetermined time interval (e.g. a 15- or 60-minute window).

This value is then multiplied by a demand charge (in $/kW). As seen in Table III, the peak-to-average ratio for the power consumed in the DR-compliant case is significantly higher than that in the no-DR case. Therefore, for our control strategy to be applicable to large consumers, further constraints on the instantaneous power consumption would have to be enforced.

V. CONCLUSION

In this work, we studied a hydronic HVAC system that serving a multi-unit residential building. We aimed to determine the optimal thermal power flow to each unit that simultaneously minimized the thermal discomfort and the power costs incurred over a time horizon based on three different energy pricing schemes. We developed mathematical expressions for modeling the temperature evolution in a residential unit over time.Finally, we used our model to run simulations to determine the optimal power consumption at each instance for given ambient temperatures and the evolution of unit temperatures for various pricing schemes. Our initial results showed that our solution may have a strong potential for saving significant electricity cost by using residential buildings for grid DR. However, for our control strategy to be applicable to large consumers who are liable to pay peak demand charge as part of their electricity bills, constraints on the maximum instantaneous power consumption would have to be enforced. Consideration of such changes in the optimal HVAC control problem is left for future work.

REFERENCES

[1] U.S. Department of Energy, "Energy savings potential and RD & D opportunities for commercial building HVAC systems," Dec. 2017, [Online] Available: https://www.energy.gov/sites/prod/files/2017/12/f46/bto-DOE-Comm-HVAC-Report-12-21-17.pdf

[2] U.S. Energy Information Administration, "Household energy use in New York: A closer look at residential energy consumption," 2019, [Online] Available: https://www.eia.gov/consumption/residential/reports/2009/state_briefs/pdf/NY.pdf

[3] M. Ali, J. Jokisalo, K. Siren, and M. Lehtonen, "Combining the demand response of direct electric space heating and partial thermal storage using LP optimization," *Electric Power System Research*, vol. 106, pp. 160-167, Jan. 2014.

[4] F. Sossan, and H. Bindner, "A comparison of algorithms for controlling DSRs in a control by price context using hardware-in-the-loop simulation," in *Proc. IEEE PES Gen. Meet.*, pp. 1-6, July 2012.

[5] M. Avci, M. Erkocand, and S. Asfour, "Residential HVAC load control strategy in real-time electricity pricing environment," in *Proc. IEEE Energytech*, pp.1-6, May 2012.

[6] "Nor'easter blasts millions with snow, wind and bitter cold," *CNN*, Jan. 2014, [Online], https://www.cnn.com/2014/01/02/us/winter-weather/index.html.

[7] "Monthly Average Price of Natural Gas - Residential," *NYSERDA*, [Online] https://www.nyserda.ny.gov/Researchers-and-Policymakers/Energy-Prices/Natural-Gas/Monthly-Average-Price-of-Natural-Gas-Residential

[8] Energy market & operational, [Online] data https://www.nyiso.com/energy-market-operational-data.

[9] K. Nakayama and R. Sharma, "Demand Charge and Response with Energy Storage," *IEEE International Conference on Communications, Control, and Computing Technologies for Smart Grids (SmartGridComm)*, pp. 1-6, Denmark, 2018.

[10] https://www.dropbox.com/s/x8zvlf0anm3iwf9/ACC2020.pdf?dl=0